PHYSICAL REVIEW B VOLUME 41, NUMBER 7 1 MARCH 1990

Ultrasonic study of crossover behavior near the chiral multicritical point of $CsNiCl_3$

M. Poirier, A. Caillé, and M. L. Plumer
Centre de Recherche en Physique du Solide et Département de Physique, Université de Sherbrooke, Sherbrooke, Québec, Canada J1K 2R1
(Received 14 September 1989)

High-resolution ultrasonic velocity measurements are used to determine magnetic phase boundary lines close to the novel multicritical point in the H-T phase diagram of $CsNiCl_3$. The results are discussed in terms of crossover behavior associated with the recently proposed chiral universality class.

The magnetic phase diagram of antiferromagnets has provided a powerful testing ground for theories of phase transitions and critical phenomena. Of particular interest is the crossover of critical behavior resulting from symmetry breaking caused by an applied magnetic field. The recent suggestion[1] of the existence of a new universality class linked to chiral degeneracy associated with fully frustrated stacked triangular layers has added to the richness of critical behavior in such systems. Among these, the quasi-one-dimensional hexagonal insulator $CsNiCl_3$ has demonstrated a variety of novel magnetic properties. Short-range antiferromagnetic correlations along the c-axis chains of Ni^{2+} ions ($S=1$) develop at temperatures below about 30 K making this material a suitable candidate for the observation of effects associated with the Haldane conjecture.[2-4] At lower temperatures, weak interchain coupling forces an effective three-dimensional (3D) magnetic system and long-range order develops below 4.86 K, followed by a second magnetic transition at 4.40 K. The magnetic phase diagram with **H** along the c axis exhibits a novel type of multicritical point which represents the intersection of one line of first-order transitions with three lines of second-order transitions,[5] as shown in Fig. 1. Mean-field Landau theory[6] and static-scaling analysis[7] have served to elucidate the universality classes involved and the importance of chirality at the spin-flop multicritical point. It is the purpose of the present high-resolution ultrasonic velocity study to examine in detail the behavior of the phase boundary lines close to the multicritical point. (Our results corroborate and extend previous ultrasonic attenuation[8] and magnetic-susceptibility data.[5]) The observed crossover behavior supports recent theoretical predictions.[7,9]

Before presenting the experimental results, it is of interest to recall the main predictions of the Landau analysis[6] and scaling theory[7] for the magnetic phase diagram. Referring to Fig. 1 (also see Fig. 1 of Ref. 6), phase 1 labels the paramagnetic state and all three of the ordered phases 2, 3, and 4 are characterized by a wave vector $\mathbf{Q}=\frac{1}{2}\mathbf{G}_{\parallel}+\frac{1}{3}\mathbf{G}_{\perp}$ (where **G** is a reciprocal-lattice vector), describing simple antiferromagnetic ordering along the c axis with an additional period-3 modulation in the basal plane. The phase boundary lines 1-2, 2-3, and 1-4 are predicted to be second-order transitions, whereas the 3-4 boundary marks the first-order spin-flop transition. The ordered phases are distinguished by the nature of the spin-polarization vector **S**. Phase 2 is collinear with $\mathbf{S}\parallel\hat{\mathbf{c}}$. Phase 3 has elliptical polarization with **S** confined to a plane including the $\hat{\mathbf{c}}$ axis, and a basal-plane crystallographic axis.[10] Of particular interest here is the spin-flop ($\mathbf{S}\perp\mathbf{H}$) phase 4 which is the so-called 120° spin structure (helical polarization) associated with triangular lattices where chiral degeneracy is responsible for the new type of universality class.[1] In materials such as $CsMnBr_3$, where this phase occurs as the zero-field ordered state, measured values of the critical exponents[11] appear to confirm these predictions.

Further understanding of the novel multicritical behavior has been found through detailed symmetry and scaling theory analyses,[7] taking into account the effects of critical fluctuations. The appropriate Ginzburg-Landau-Wilson Hamiltonian can be expressed as[6,7]

$$\mathcal{H}=(\nabla\mathbf{a})^2+(\nabla\mathbf{b})^2+r(\mathbf{a}^2+\mathbf{b}^2)+u(\mathbf{a}^2+\mathbf{b}^2)^2 +v[(\mathbf{a}\cdot\mathbf{b})^2-\mathbf{a}^2\mathbf{b}^2]-g(\mathbf{a}^2+\mathbf{b}^2-3a_z^2-3b_z^2)\,, \quad (1)$$

$$r=r_0+em^2+g\,, \quad (2)$$

$$g=\tfrac{1}{3}(fm^2-\delta)\,, \quad (3)$$

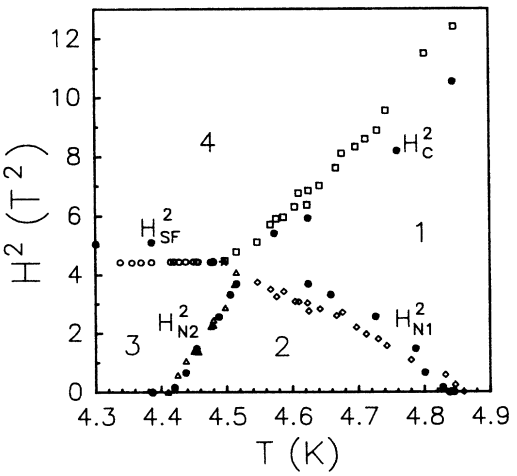

FIG. 1. Magnetic phase diagram as determined from sound-velocity anomalies (H_{sf}, open circles; H_C, squares; H_{N1}, diamonds; H_{N2}, triangles) along with previous susceptibility data (Ref. 5) (solid circles). Asterisk denotes the multicritical point. Labeled regions 1-4 refer to paramagnetic, linear, elliptical, and helical phases, respectively.

where $r_0 = a(T - T_Q)$, $\mathbf{m}$ is the uniform magnetization induced by the magnetic field applied along the c axis, and $\mathbf{a}$, $\mathbf{b}$ are defined through the spin density by

$$\mathbf{s}(\mathbf{r}) = \mathbf{m} + \mathbf{a}\cos(\mathbf{Q}\cdot\mathbf{r}) + \mathbf{b}\sin(\mathbf{Q}\cdot\mathbf{r}) , \quad (4)$$

and related to the spin-polarization vector[6] by $\mathbf{a} = 2\,\mathrm{Re}\mathbf{S}$ and $\mathbf{b} = -2\,\mathrm{Im}\mathbf{S}$. Note that the wave vectors $+\mathbf{Q}$ and $-\mathbf{Q}$ give rise to two inequivalent spin structures (e.g., right- and left-handed helicity in phase 4). A comparison of the mean-field analysis[6] with experimental data leads to the results that the coefficients δ, f, u, and v are positive, whereas e is negative. The terms g and v in Eq. (1) are responsible for breaking the isotropy in extended $2n$ spin space. For $g = v = 0$, the critical behavior would be that of a $2n$-component isotropic Heisenberg model ($n = 3$). If v were negative, this term would favor a linearly polarized state ($a = 0$ or $b = 0$) (Ref. 10) and lead to usual bicritical-point behavior in the magnetic phase diagram.[12,13] In the present case ($v > 0$), a helical configuration with $\mathbf{a} \perp \mathbf{b}$, is stabilized by the v term giving rise to additional structure to the order-parameter space and the chiral behavior.[1] The *sign* of the coefficient g of the quadratic term is field dependent creating easy-axis anisotropy ($g < 0$) at low fields and easy-plane anisotropy ($g > 0$) at high-field values. It is the competition between these two terms (v and g) which yields the rich phase diagram of $CsNiCl_3$.

The three second-order transition lines of Fig. 1 merging at the multicritical point (T_m, H_m) correspond to nonzero values of g and their criticalities are predicted[7] to be the following: (i) the 1-2 phase boundary is associated with the xy universality class involving the spin components a_z and b_z; (ii) the 2-3 boundary also has xy criticality involving either (b_x, b_y) or (a_x, a_y) depending on whether a_z or b_z is chosen to be nonzero by symmetry breaking at the 1-2 phase boundary; (iii) the 1-4 phase boundary has critical properties associated with the $n = 2$ chiral universality class involving (a_x, a_y) and (b_x, b_y). The point $r = 0$ and $g = 0$ in the phase diagram corresponds to the multicritical point where the system has recovered the full isotropy in spin space and its criticality is expected to be governed by the new $n = 3$ chiral fixed point.[1] g is the scaling field at the chiral fixed point and the singular part of the free energy around the multicritical point is written in the standard scaling form as[7,12,14,15]

$$F_s(\tilde{t}, \tilde{g}) \cong |\tilde{t}|^{2-\alpha} \mathcal{F}(\tilde{g}/|\tilde{t}|^{\phi}) , \quad (5)$$

where the linear scaling fields $\tilde{t}$ and $\tilde{g}$ are given by

$$\tilde{t} = t + qh^2 , \quad \tilde{g} = h^2 - pt , \quad (6)$$

with $t = (T - T_m)/T_m$ and $h^2 = H^2 - H_m^2$. The quantity p, the limiting tangent of the spin-flop line, is $T_m(dH_{sf}^2/dT)_m$; q is more difficult to estimate[15] but a mean-field value can be obtained by comparing (6) with (2). The specific-heat exponent α and crossover exponent ϕ are those associated with the $n = 3$ chiral fixed point. ϕ is expected to be greater than unity and a recent numerical estimate of Kawamura[9] based on the two-loop renormalization-group calculation gives a value of $\phi \cong 1.06$.

The extended scaling hypothesis included in Eq. (5) implies that the three critical-phase boundary lines must satisfy

$$\tilde{g}/|\tilde{t}|^{\phi} = w_i , \quad (7)$$

where the w_i are constants with $i = N1$, $N2$, and C corresponding to the phase boundaries 1-2, 2-3, and 1-4, respectively. Near the multicritical point one can then write

$$H_i^2 - H_m^2 \cong pt + w_i|t + q(H_i^2 - H_m^2)|^{\phi} + A_i t . \quad (8)$$

The terms $A_i t$ are present in mean-field theory[6,12] and are the leading correction to the scaling field $\tilde{g}$. The comparison of Landau theory[6] with experimental data gives the results that A_{N2} and A_C are positive, whereas A_{N1} is negative.

The principal significance of the above results relevant to the present experimental study can be summarized succinctly. Since $\phi \gtrsim 1$, the three critical lines H_{N1}^2, H_{N2}^2, and H_C^2 are predicted to approach the multicritical point tangentially. Results of the ultrasonic velocity measurements summarized below support this general feature and show additional effects attributed to critical fluctuations.

The ultrasonic velocity was measured with a pulsed acoustic interferometer whose operating principle is based on the measurement of the phase difference between the ultrasonic wave and a reference signal.[16] For normal operating conditions, this phase difference is inversely proportional to the ultrasonic velocity v according to the relation

$$\phi = 2\pi f(2nL)/v , \quad (9)$$

where n, L, and f are, respectively, the number of back-and-forth trips executed by the acoustic pulse, the sample's length, and the frequency. If the phase difference is maintained constant during the experiment, the relative velocity variation is given by

$$\Delta v/v = \Delta f/f + \Delta L/L . \quad (10)$$

If the linear thermal-expansion coefficient may be neglected, the changes in the ultrasonic velocity are directly proportional to the frequency variations.

The single crystal used for this experiment was grown by the Bridgman method. Its tendency to cleave along the {1120} plane facilitated its orientation for acoustic propagation along the c axis [0001]. Parallel faces, approximately 10 mm apart with normals parallel to the c axis, were polished to receive the acoustic transducers. The longitudinal acoustic pulses are generated, at 30 MHz and odd overtones, by 36° Y-cut co-axially plated $LiNbO_3$ piezoelectric transducers bonded to the sample with GE Silicone Sealant. The rf signal is fed to the transducers by a HP-8340B Synthesized Sweeper through pin diode switches. The phase difference is obtained after mixing the acoustic signal with a reference one; it is maintained constant by an automatic adjustment of the synthesized frequency. A precision better than 1 ppm is easily obtained with this interferometer.

The longitudinal ultrasonic signals were obtained at 30, 90, 150, and 210 MHz with the propagation direction along the c axis; no frequency dependence was observed over the 2–10 K temperature range. All the results re-

ported here were obtained in transmission at 90 MHz with the magnetic field also applied parallel to the c axis.[17] The sample temperature was monitored with silicon diode and $SrTiO_3$ capacitance (practically magnetic-field independent) sensors and stabilized with a Lakeshore DRC-93C controller. With the capacitance sensor a stabilization better than 6 mK was achieved during the magnetic-field sweeps (0–9 T). The relative thermal expansion of $CsNiCl_3$ along the c axis[18] is at least 1 order of magnitude smaller than the relative frequency variations measured in this experiment for $T < 6$ K. It will thus be neglected and the frequency variations are directly translated into velocity or elastic modulus changes; for a longitudinal wave propagating along the c axis $\Delta v/v = \frac{1}{2}\Delta C_{33}/C_{33}$.

The measured temperature dependence of $\Delta C_{33}/C_{33}$ for $2 < T < 10$ K is similar to that reported by Mountfield and Rayne.[19] The onset of three-dimensional antiferromagnetic ordering is seen as a small continuous slope variation occurring at $T_{N1} \cong 4.86$ K while the transverse spin ordering manifests itself at $T_{N2} \cong 4.41$ K as a pronounced anomaly. The overall modulus variation measured in our experiment is, however, four times larger than the measurement of Mountfield and Rayne at 10 MHz; as indicated above, no frequency dependence has been observed between 30 and 210 MHz.

Our ultrasonic velocity data for H∥ĉ are summarized in Fig. 1 as a H^2-T phase diagram where the magnetic phases and boundary lines are labeled as in Ref. 6. Each point of Fig. 1 was obtained from a plot of $\Delta v/v$ vs H^2 at constant temperature. A few examples of such plots are presented in Figs. 2 and 3 for selected temperatures between 4.42 and 5.59 K. In Fig. 2, H_{N1} and H_{N2} are determined by a slope variation on the high-field side of the transition, being quite pronounced in the case of H_{N2}; in Fig. 3, H_{sf} and H_c are instead fixed by the zero-slope field in the region of maximum velocity variation. The way by which each field is determined is suggested by the nature of the particular transition line. The different character exhibited by these four sets of data reflects the different

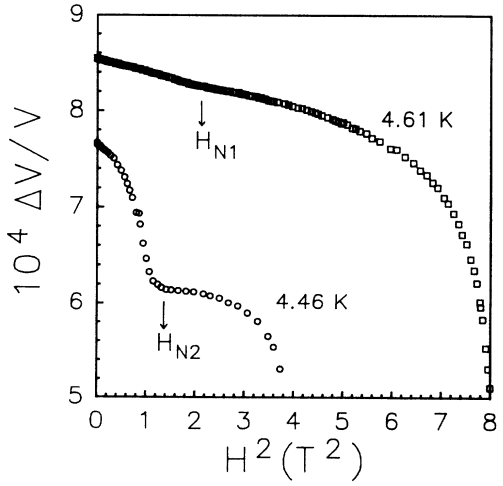

FIG. 2. Relative sound velocity as a function of H^2 at T = 4.46 and 4.61 K.

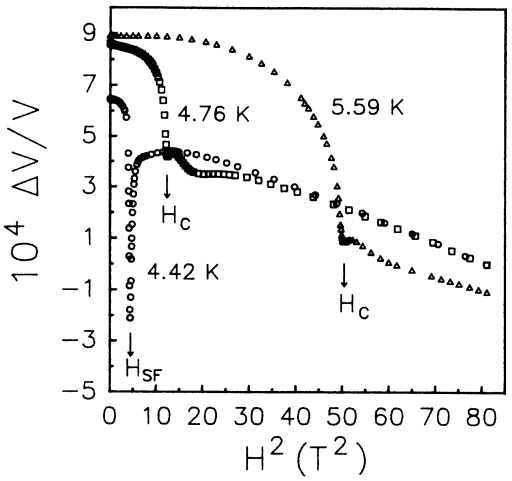

FIG. 3. Relative sound velocity as a function of H^2 at T = 4.42, 4.76, and 5.59 K.

type of magnetic orderings involved in the associated phase transitions. We note that these results are in contrast with the predictions of the Landau theory[20] for the field dependence of $\Delta C_{33}/C_{33}$ which gives a simple discontinuity at a phase transition and H^2 behavior close to the anomaly. The relative weakness of the slope variation at H_{N1} is consistent with the small anomaly observed in the $H = 0$ temperature scans of $\Delta C_{33}/C_{33}$ discussed above but is puzzling in view of the pronounced anomalies observed in thermal expansion[18] and specific heat[21] measurements. A recent study[22] of critical fluctuation effects on sound-velocity anomalies at phase transitions may be relevant for an understanding of these results. The dramatic singular behavior observed at the spin-flop field H_{sf} is attributed to the first-order nature of this phase transition and contrasts with magnetostriction data[23] where only a small slope change in $\Delta L/L$ is seen. The possibility that the 1-4 boundary at H_c is in fact a first-order transition cannot be excluded in view of the data of Fig. 3.

In addition to providing a verification of the novel multicritical-point behavior suggested by the previous susceptibility measurements[5] and mean-field analysis,[6] our more detailed data in Fig. 1 show some effects due to critical fluctuations and crossover behavior in support of theoretical prediction. The values of T_m and H_m^2 are estimated to be 4.495 K and 4.430 T^2, respectively, which differ from the previous crude estimates[6] of 4.6 K and 5.3 T^2. The apparent lowering of T_m relative to its mean-field-like value is expected;[12,15] however, the origin of the discrepancy in the values for H_m^2 is not clear. Since the predicted value of ϕ is very close to unity, the tangential convergence of the critical lines at T_m, H_m^2 is expected to be obscure; this is evident in the data for H_{N1}^2 and H_C^2. (Larger values of ϕ are associated with usual bicritical and tetracritical phenomena.[12]) The dramatic turnover of H_{N2}^2 on approaching the multicritical point, however, provides clear evidence of departure from mean-field behavior and support for the prediction that H_{N1}^2 and H_{N2}^2 scale with the same exponent ϕ. A detailed numerical fit of the data for H_{N1}^2 and H_C^2 to the predicted form Eq. (8) was attempted but with somewhat unsatisfactory results due

to scatter in the data. This analysis does show, however, that ϕ is very close to unity in agreement with the prediction.

In conclusion, these high-resolution ultrasonic velocity measurements have served to elucidate the novel multicritical behavior in the magnetic phase diagram of $CsNiCl_3$. The predicted convergence of a spin-flop line with three critical transition lines has been verified and contrasts with usual bicritical and tetracritical points. Critical fluctuations associated with this multiphase point are expected to be governed by the recently exposed $n=3$ chiral universality class. Our results support the predictions that the three critical lines scale with the same crossover exponent and that ϕ is very close to unity. Further experimental investigation of related systems (e.g., $RbNiCl_3$, $CsNiBr_3$, $CsMnI_3$) which are expected to exhibit a similar type of magnetic phase diagram is desirable.

We thank K. Hirakawa and W. J. L. Buyers for the crystal and M. Castonguay for technical assistance. This work was supported by the Natural Sciences and Engineering Research Council of Canada and le Fonds Formation de Chercheurs et l'Aide à la Recherche du Gouvernement du Québec.

[1]H. Kawamura, J. Appl. Phys. **63**, 3086 (1988); Phys. Rev. B **38**, 4916 (1988); J. Phys. Soc. Jpn. **58**, 584 (1989).

[2]W. J. L. Buyers, R. M. Morra, R. L. Armstrong, M. J. Hogan, P. Gerlach, and K. Hirakawa, Phys. Rev. Lett. **56**, 371 (1986); R. M. Morra, W. J. L. Buyers, R. L. Armstrong, and K. Hirakawa, Phys. Rev. B **38**, 543 (1988).

[3]M. Steiner, K. Kakurai, J. K. Kjems, D. Petitgrand, and R. Pynn, J. Appl. Phys. **61**, 3953 (1987).

[4]I. Affleck, Phys. Rev. Lett. **62**, 474 (1989).

[5]P. B. Johnson, J. A. Rayne, and S. A Friedberg, J. Appl. Phys. **50**, 1853 (1979).

[6]M. L. Plumer, K. Hood, and A. Caillé, Phys. Rev. Lett. **60**, 45 (1988); **60**, 1885(E) (1988).

[7]H. Kawamura, A. Caillé, and M. L. Plumer, this issue, Phys. Rev. B **41**, 4416 (1990).

[8]D. P. Almond and J. A. Rayne, Phys. Lett. **55A**, 137 (1975).

[9]H. Kawamura (unpublished).

[10]X. Zhu and M. B. Walker, Phys. Rev. B **36**, 3830 (1987).

[11]T. E. Mason, B. D. Gaulin, and M. F. Collins, Phys. Rev. B **39**, 586 (1989); B. D. Gaulin, T. E. Mason, M. F. Collins, and J. Z. Larese, Phys. Rev. Lett. **62**, 1380 (1989).

[12]J. M. Kosterlitz, D. R. Nelson, and M. E. Fisher, Phys. Rev. B **13**, 412 (1976).

[13]M. L. Plumer, A. Caillé, and K. Hood, Phys. Rev. B **39**, 4489 (1989).

[14]A. D. Bruce and A. Aharony, Phys. Rev. B **11**, 478 (1975).

[15]M. E. Fisher, Phys. Rev. Lett. **34**, 1634 (1975).

[16]G. Gorodetshy and I. Lachterman, Rev. Sci. Instrum. **52**, 1387 (1981).

[17]Some field misalignment is unavoidable. The principal effect within mean-field theory would be to shift the apparent multicritical point to a slightly higher temperature.

[18]J. A. Rayne, J. G. Collins, and G. K. White, Solid State Commun. **33**, 39 (1980).

[19]K. R. Mountfield and J. A. Rayne, J. Phys. (Paris) Colloq. **42**, C6-468 (1981).

[20]Following, e.g., the procedure discussed by M. L. Plumer and A. Caillé, Phys. Rev. B **37**, 7712 (1988).

[21]S. J. Collocott and J. A. Rayne, J. Appl. Phys. **61**, 4404 (1987).

[22]L. Benguigui and P. Martinoty, Phys. Rev. Lett. **63**, 774 (1989).

[23]J. A. Rayne, J. G. Collins, and G. K. White, J. Appl. Phys. **55**, 2404 (1984).